Journal of Energetic Materials
Publication details, including instructions for authors and subscription information:
http://www.informaworld.com/smpp/title~content=t713770432

Numerical Simulation of Experiments on the Low-Velocity Impact on HMX-Based HE Using Explosive Transformation Initiation Kinetics

A. R. Gushanov[a]; N. A. Volodina[a]; G. V. Belov[a]; V. N. Khvorostin[a]; D. M. Isheev[a]
[a] Russian Federal Nuclear Center—All-Russia Research Institute of Experimental Physics, Sarov, Russia

Online publication date: 15 October 2010

To cite this Article Gushanov, A. R. , Volodina, N. A. , Belov, G. V. , Khvorostin, V. N. and Isheev, D. M.(2010) 'Numerical Simulation of Experiments on the Low-Velocity Impact on HMX-Based HE Using Explosive Transformation Initiation Kinetics', Journal of Energetic Materials, 28: 1, 50 — 65
To link to this Article: DOI: 10.1080/07370651003720429
URL: http://dx.doi.org/10.1080/07370651003720429

Journal of Energetic Materials, 28: 50–65, 2010

ISSN: 0737-0652 print/1545-8822 online
DOI: 10.1080/07370651003720429

Numerical Simulation of Experiments on the Low-Velocity Impact on HMX-Based HE Using Explosive Transformation Initiation Kinetics

A. R. GUSHANOV, N. A. VOLODINA, G. V. BELOV, V. N. KHVOROSTIN, and D. M. ISHEEV

Russian Federal Nuclear Center—All-Russia Research Institute of Experimental Physics, Sarov, Russia

This article presents a model of explosive transformation initiation under low-velocity impacts. It also describes 2D simulation by the LEGAK-3D code system of two series of experiments on impacting samples of HMX-based high explosive (HE) by a spherical fragment of mass 12 g and by an impactor of mass 2.76 kg and presents results of computations. The model was verified during the computational process, and a single set of parameters was selected to describe all experiments. The numerical simulation results are in satisfactory agreement with experimental data, both in the description of the explosive transformation initiation conditions and in the description of their evolution.

Keywords: initiation, low-velocity impact, numerical simulation

Address correspondence to A. R. Gushanov, Russian Federal Nuclear Center—All-Russia Research Institute of Experimental Physics, Sarov, Russia. E-mail: a.r.gushanov@gmail.com

Model of Explosive Transformation Initiation

Description of experiments on low-velocity initiation of explosive transformations is a problem of great interest in both theory and practice. There is a practical need for a model that would predict conditions for explosive transformation initiation. Such a model should be based on a physical mechanism of the explosive transformation initiation process and should be able to describe results of different experiments on low-velocity impact with the impactor mass varying from 12 g to 10 kg and the impact-to-initiation time varying within the range from 50 to 500 μs.

Bakhrakh et al. [1,2] considered in detail the microscopic-level processes in explosives under low-velocity impacts. It has been shown that material straining is a heterogeneous process, and there are dissipation areas in which the strain rate is higher than in the bulk material and the total energy dissipated due to viscous–plastic straining is concentrated. Heterogeneity of the strain rate and mechanical energy dissipation rate leads to heterogeneity of the temperature field. Temperature in a dissipation area will significantly exceed the temperature of the material surrounding such an area. Due to the heterogeneity of the temperature field the chemical reaction and associated energy release starts not in the whole high explosive (HE) volume at one time, but it is initiated in dissipation areas, which transform into hot spots (areas of hot material entering into the chemical reaction) upon achievement of some chemical reaction rate.

The assertion of heterogeneous strain and generation of shear bands even under homogeneous loading of material is not new; the existence of such structures in metals is a well-known fact (see Nozovtsev et al. [3] and Daridon et al. [4]). Some other authors [5–7] also reported that initiation of explosive transformations in HE under low-velocity impacts is due to straining in shear bands. The result of studying processes in an explosive under low-velocity impact was a model of explosive transformation initiation [2]. Numerical simulation of the Steven test (see Bakhrakh et al. [2]) type experiments with explosive PBX 9501 was performed using this model. These simulations

demonstrate that numerical simulation of conditions, under which explosive transformations are initiated, is feasible. Later, the model was improved by taking into account some physical processes whose contribution had not been considered earlier. The processes, such as material cooling in dissipation areas due to heat transfer and possible turbulance of the molten material flow in dissipation areas, were additionally taken into account. In addition, the experimentally proved fact of incomplete material burnup under low-velocity impact was taken into account.

The modified equations look like

$$\frac{dE'}{dt} = \frac{1}{\rho^{1-\varepsilon}} \frac{\left(\Delta_{ik}^2\right)^{1+\varepsilon/2}}{2^{1+\varepsilon/2}\alpha^{2-\varepsilon}} h^{2\varepsilon} \cdot \eta^{1-\varepsilon} + \frac{E_- - E'}{\alpha} \frac{d\alpha}{dt} - \frac{1}{\rho\alpha h^2} a_2 \kappa \frac{T_M - T_0}{(1-\alpha)} + Q\frac{d\lambda'}{dt} \tag{1}$$

$$\frac{d\alpha}{dt} = \frac{\kappa}{E_M \rho h^2} \left(a_1 \frac{T' - T_M}{\alpha} - a_2 \frac{T_M - T_0}{(1-\alpha)} \right) \tag{2}$$

$$\frac{d\lambda'}{dt} = (1-\lambda') B e^{-\frac{E_a}{RT'}} \tag{3}$$

$$\frac{d\lambda}{dt} = \begin{cases} \frac{1}{\tau_r} \frac{(\lambda_E - \lambda)}{\lambda_E}, & \lambda' > \lambda'_0 \\ 0, & \lambda' < \lambda'_0 \end{cases} \tag{4}$$

Here, quantities marked with the symbol $'$ characterize the material state in dissipation areas (incipient hot spots): E' is the internal energy of material, T' is the material temperature, λ' is the mass concentration of reaction products, ρ is density, α is the mass fraction of material in dissipation areas, Q is the HE caloricity, and η is the dynamic viscosity factor of material in dissipation areas. $\Delta_{ik} = \frac{\partial v_i}{\partial x_k} + \frac{\partial v_k}{\partial x_i} - \frac{2}{3}\delta_{ik}\frac{\partial v_l}{\partial x_l}$ is the strain rate tensor, and λ is the macroscopic mass concentration of reaction products. Quantities τ_r, λ'_0, h, κ, a_1, a_2, ε, λ_E are the model parameters. $E = C(T_M - T_0)$ is the internal energy of solid heated to its melting point.

Equation (1) describes the energy conservation law and determines the specific internal energy of material in dissipation areas. The start time of calculations of the values of E' for each point is determined by the start time of plastic strain of material in the vicinity of each point. The first term in the right-hand part of the equation describes material heating due to viscous dissipation of energy, the second term describes the specific internal energy decrease with growth of dissipation areas, the third term describes energy decrease due to heat flow to the material surrounding dissipation areas, and the fourth term describes the energy increase during the chemical reaction. Equation (2) describes the dissipation area growth rate. Equation (3) describes the rate of chemical reaction in a dissipation area according to the Arrhenius law. Equation (4) describes the hot spot growth rate and thereby describes the energy release on a macroscopic scale.

The model offered in the article uses many parameters. However, many of them are not parameters of the model proper; they characterize processes independent of the model (viscosity of material, Arrhenius kinetics parameters, etc.). The model parameters are, as follows: α_0 is the initial mass fraction of material contained in dissipation areas, h is the distance between neighboring dissipation areas, a_1 and a_2 are empiric parameters determining the heat transfer contribution to cooling the dissipation area material, ε is an empiric parameter determining the degree of material flow turbulance in dissipation areas, λ_E is the maximum degree of HE burnup, and τ_r is the burnup time of material between hot spots. Parameters α_0, h, a_1, a_2, and ε determine conditions under which explosive transformations are initiated; parameters λ_E and τ_r determine the behavior of evolution of these conditions. In the calculations described below the following set of the initiation model constants was used: $\alpha_0 = 0.635 \times 10^{-3}$, $\tau_r = 300$ μs, $\lambda'_0 = 0.9$, $a_1 = 4 \cdot 10^{-4}$, $a_2 = 0$, $\varepsilon = 0$, $h = 0.02$ cm, $\lambda_E = 0.1$.

The calculations described in the article were carried out using LEGAK codes [8].

Initiation of Explosive Transformations by Impact of a Spherical Fragment

During experiments at RFNC-VNIIEF the threshold velocity was determined for initiation of explosive transformations in an octogen-based HE under the impact of a steel-made spherical fragment. A steel ball of diameter 14.3 mm and weight 12 g accelerated by a projectile device impacted a cylindrical HE cartridge of diameter 120 mm, thickness 60 mm, and mass 1,280 g. The back-plane surface of the cartridge had a detecting plate made of steel. A schematic diagram of the experiment is given in Fig. 1. During these experiments the impactor velocity, the time of impact, and the times of the detecting plate arrival at

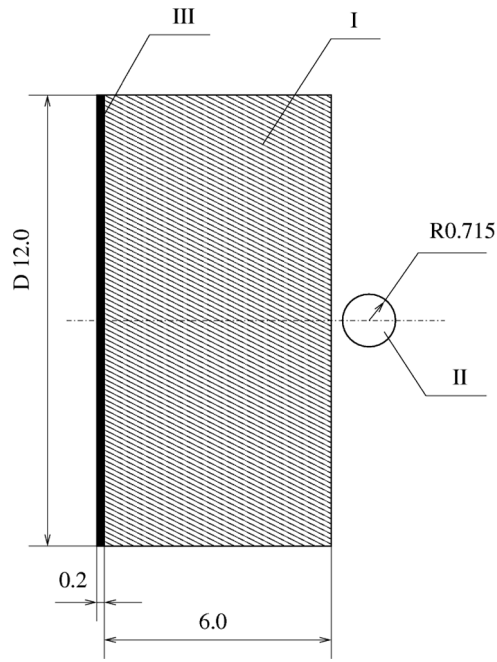

Figure 1. Schematic diagram of experiments to find the threshold velocity at which explosive transformations are initiated by impact with a ball. (I) HE, (II) a steel ball, and (III) a detecting plate.

contact pickups on bases 2, 7, 12, 22, and 32 mm were measured. After the experiments the surrounding entities demonstrated tracks of HE not entered into the chemical reaction.

Computations were carried out using a Eulerian (static) computational grid with $h = 0.02$ cm. About 200,000 computation points were used. Elastic–plastic approximation was used to describe materials. Low-velocity simulations pose a special requirement for the prevention of computational perturbations—in particular, perturbations of the velocity field—because the development of such perturbations affects the value of the second invariant of the strain rate tensor, which is used as a criterion of HE initiation under low-velocity impact. The velocity field typical for LEGAK codes was smoothed during computations.

Experiments with impact velocities 37.2, 49.2, 52.25, 59.7, and 105.37 m/s were simulated. The calculated threshold velocity of explosion initiation agrees with the experimental value: with velocity 49.2 m/s transformations are not initiated in calculations or in experiments; with velocity 52.2 m/s an explosion takes place in experiments and according to the results of calculations. Table 1 gives the main results of calculations, namely, the time before the ball rebounds, that is, reverses direction; the maximum temperature and degree of material burnup in dissipation areas at the ball rebound time; times of explosive transformation initiation; and depth of a crater created by the ball (in experiment and in calculations). Figure 2 illustrates maximum temperature in dissipation areas as a function of time with impact velocities 37.2, 49.2, 52.25, 59.7, and 105.37 m/s. As one can see from these figures, with impact velocities below the threshold value (52.25 m/s) material is heated in dissipation areas; however, such heating is insufficient to initiate a self-sustaining chemical reaction with energy release. It is heating the material of the dissipation areas to the required temperature that creates the necessary conditions for initiation of explosive transformations.

Figure 3 illustrates fields for the second invariant of the strain rate tensor (in units $1/[10\,\mu\text{s}]^2$), material temperature (K), and mass fraction of reaction products in dissipation areas for

Table 1
Main results of numerical simulation of experiments to find the threshold velocity of impacting with a ball to initiate explosive transformations

Velocity of impact (m/s)	Ball rebound time (μs)	Maximum temperature in dissipation areas at the ball rebound time (K)	Maximum degree of burnup in dissipation areas at the ball rebound time	Time of explosive transformation initiation (μs)	Depth of crater (mm)	
					Experiment	Simulations
37.2	60	764	$2.94 \cdot 10^{-3}$		1.5	1.6
49.2	60	804	$8.05 \cdot 10^{-3}$		2.2	2
52.25	60	827	$1.24 \cdot 10^{-2}$	100		
59.7				45		
105.37				15		

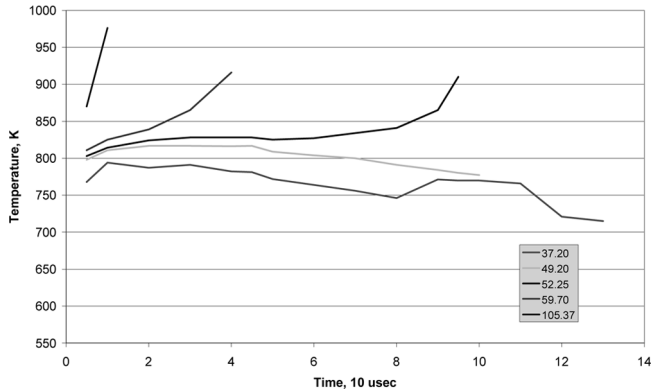

Figure 2. Maximum temperature in dissipation areas as a function of time for velocities 37.2, 49.2, 52.25, 59.7, and 105.37 m/s.

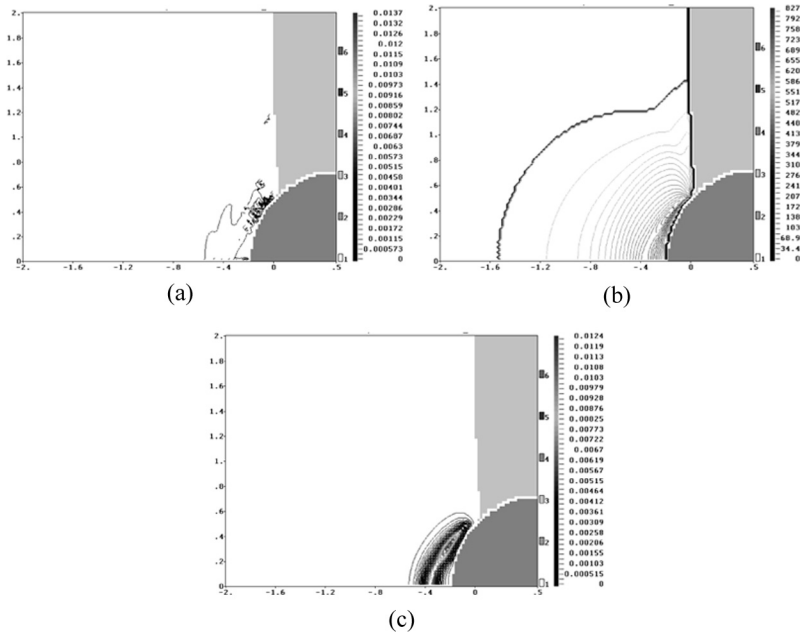

Figure 3. The second invariant of the strain rate tensor (left), temperature (center), and burnup (right) in dissipation areas for computations with impact velocity 52.25 m/s at time $t = 60\,\mu$s.

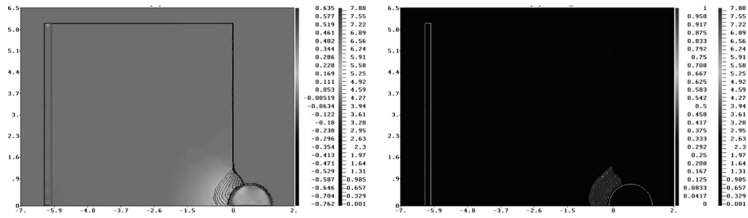

Figure 4. Pressure field (left) and burnup field (right) with density isolines for computations with impact velocity 52.25 m/s at time $t = 130\,\mu$s.

computations with impact velocity 52.25 m/s at time $t = 60\,\mu$s. As one can see, the initiation spot (an area with maximum temperature in dissipation areas) is generated at a distance of about 0.1 cm to the HE/impactor interface and at a distance of 0.35 cm to the impact axis. Figure 4 illustrates field of pressures (HPa) and fields of mass fractions of EP in dissipation areas with isolines of density (g/cm^3) for computations with impact velocity 52.25 m/s at time $t = 130\,\mu$s. Figure 5 illustrates how the time of closure of electrocontact pickups with a

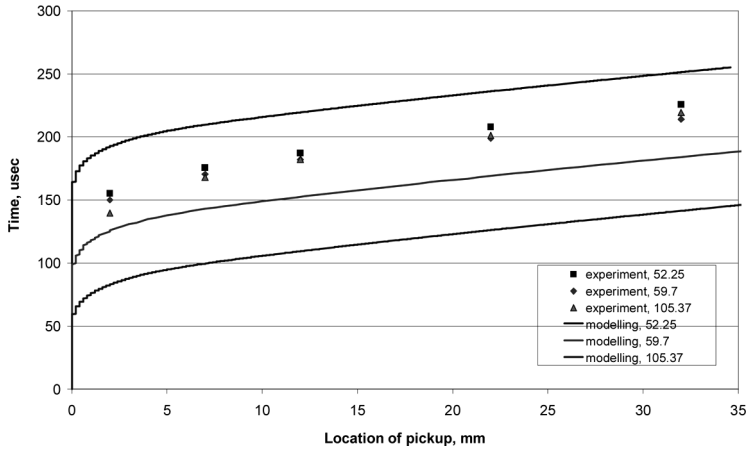

Figure 5. Curves of contact pickup operation times versus locations of pickups for experiments and computations with impact velocities 52.25, 59.7, and 105.37 m/s.

detecting plate depends on locations of these pickups both in experiments and computations with impact velocities 52.25, 59.7, and 105.37 m/s. As one can see, there is a good agreement between experiment and computations in the flight dynamics of the plate. However, there is a difference between experiments and computations in the plate motion start times. In experiments, this time weakly depends on the impact velocity, but computation results demonstrate a noticeable difference between the plate motion start times with impact velocities 52.25, 59.7, and 105.37 m/s. The behavior of these dependences is the same in experiments and computations: a higher impact velocity leads to less delay in the plate motion start.

Explosive Transformation Initiation by Impact of a 2.76 Kg Projectile

During experiments at RFNC-VNIIIEF the threshold velocity for initiation of explosive transformations in a prototype octogen-based HE was measured for impact by a round-nosed projectile. The test charge consisted of an HE disk of diameter 120 mm and thickness 13.5 mm placed in a steel shell. A schematic diagram of the assembly with HE and projectile is shown in Fig. 6. The projectile had a round nose with a 22-mm radius and weighed 2.79 kg. Three experiments were conducted.

In an experiment with projectile velocity 42.1 m/s we observed an explosion that resulted in complete destruction of the assembly shell and deformation of the target support. In experiments with projectile velocity 29.1 m/s no explosion was observed, a hollow appeared in HE and the radial gap between the prototype HE and the assembly shell was completely filled with explosive displaced from the impact place. In an experiment with projectile velocity 32.4 m/s we observed an explosion that resulted in complete destruction of the assembly shell and deformation of the target support fragments.

The main results of computations (the time before the impactor rebounds; that is, reverses direction, maximum temperature, and burnup in dissipation areas at the impactor rebound time, time of initiating explosive transformations,

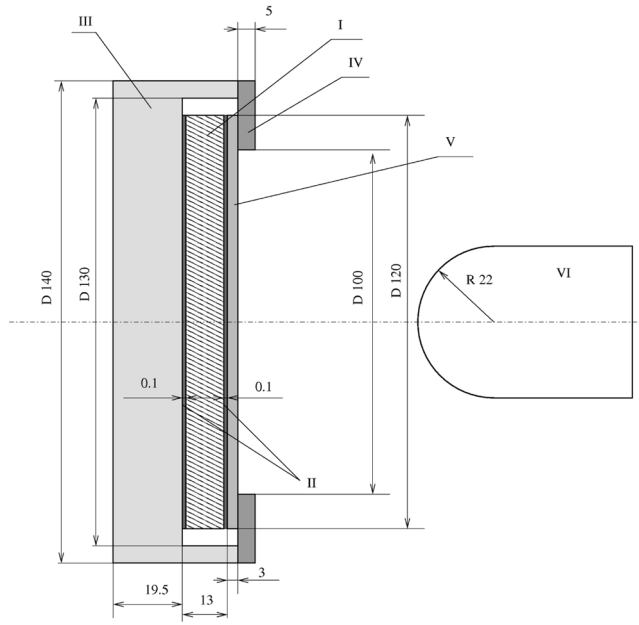

Figure 6. Schematic diagram of the experimental design used to study explosive transformation initiation by impact of a 2.76 kg projectile. (I) A prototype HE, (II) Teflon pads, (III) a steel shell, (IV) a steel disk, (V) a steel cover, and (VI) a steel impactor.

depth of crater) are given in Table 2. As one can see, the calculated results agree with experimental data for impact velocities 29.1 and 42.1 m/s; with impact velocity 29.1 m/s both experiments and computations demonstrated no explosion; with impact velocity 42.1 m/s an explosion was observed in experiments and in results of computations. With impact velocity 32.4 m/s, an explosion was observed in experiments; however, calculations do not predict explosive transformations. Figure 7 shows maximum temperature in dissipation areas as a function of time for impact velocities 29.1, 32.4, and 42.1 m/s. Similar to impact with a spherical fragment, it can be seen that material heating in dissipation areas to the required temperature creates the necessary conditions for initiation of explosive transformations.

Table 2
Main results of numerical simulation of experiments on explosive transformation initiation by impact of a 2.76 kg projectile

Velocity of impact (m/s)	Impactor rebound time (μs)	Maximum temperature in dissipation areas at the impactor rebound time (K)	Maximum degree of burnup in dissipation areas at the impactor rebound time	Explosive transformation initiation time (μs)	Depth of crater (mm)
29.1	560	675	$1.11 \cdot 10^{-3}$		9.5
32.4	570	689	$2.17 \cdot 10^{-3}$		10.8
42.1				380	

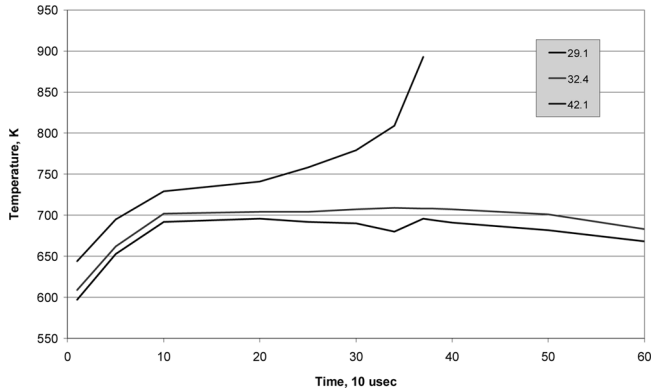

Figure 7. Curves of maximum temperature in dissipation areas as a function of time for impact velocities 29.1, 32.4, and 42.1 m/s.

Figure 8 illustrates field of the second invariant of the strain rate tensor (in units $1/[10\,\mu s]^2$), material temperature (K), and mass fraction of reaction products in dissipation areas for computations with impact velocity 42.1 m/s at time 250 μs. The strain rate and temperature of material and degree of burnup in dissipation areas achieve their maximum values in the area located on the impact axis. Figure 9 illustrates fields of pressure (HPa) and mass fraction of reaction product in dissipation

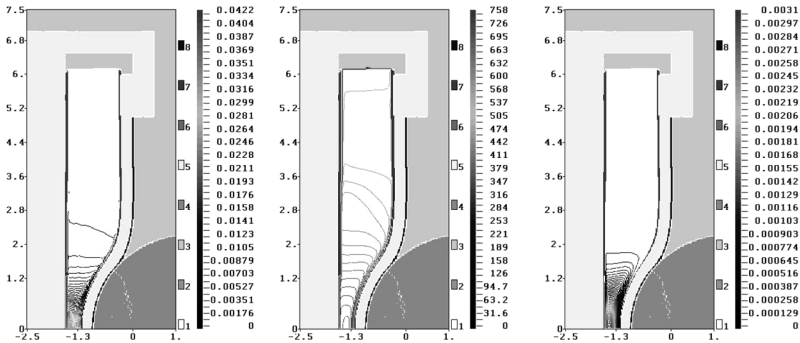

Figure 8. The second invariant of strain rate tensor (left), temperature (center), and burnup (right) in dissipation areas for computations with impact velocity 42.1 m/s at time 250 μs.

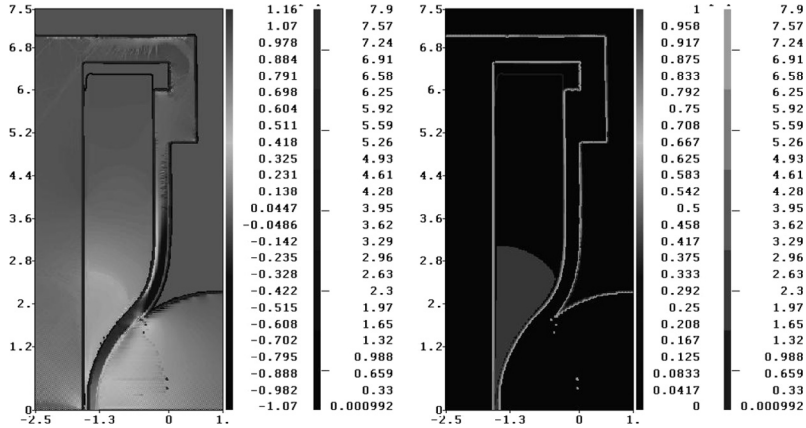

Figure 9. Pressure field (left) and burnup field (right) in dissipation areas with density isolines for computations with impact velocity 42.1 m/s at time 440 μs.

areas with isolines of density (g/cm^3) for computations with impact velocity 42.1 m/s at time 440 μs.

Conclusion

Results of the numerical simulation of conditions for initiation of explosive transformations under impact of a spherical fragment of mass 12 g on an octogen-based HE are in good agreement with experimental data: the threshold impact velocity for explosive transformation initiation is within the range 49.2 to 52.25 m/s in computations and experiments. The flight dynamics of a detector plate predicted in computations and describing the propagation and parameters of the released energy wave is close to that observed in experiments.

Results of numerical simulation of experiments on initiation of explosive transformations by impacting with a 2.76 kg projectile agree, in part, with experimental data: with impact velocity 29.1 m/s both computations and experiment did not demonstrate initiation of explosive transformations, and with impact velocity 42.1 m/s explosive transformations were initiated both in calculations and in experiments; however, with impact

velocity 32.4 m/s initiation of explosive transformations was observed experimentally, but it was not predicted by computations.

One of the possible causes of such results is that the model of HE straining and fracturing used for computations was not absolutely adequate. It is also possible that initiation of explosive transformations is a probabilistic process; that is, some parameters (small discrepancy in HE density and sensitivity, deviation of impactor from the assembly axis, etc.), which are beyond its result with which are currently beyond control in the experiments may influence the result (initiation of explosive transformations or its absence). Continued numerical simulation using a more adequate strain model and experimental investigations that could allow, in particular, understanding the role of probabilistic processes in initiating explosive transformations under low-velocity impact is planned.

References

[1] Bakhrakh, S. M., N. A. Volodina, and A. R. Gushanov. 2005. Initiation of solid HE detonation under low-velocity impacts: The physical model and numerical simulation. In *''Youth in Science'': A Book of Presentations at the IVth Science and Technology Conference*. Sarov.

[2] Bakhrakh, S. M., N. A. Volodina, and A. R. Gushanov. 2006. Numerical simulation of explosive transformation initiation in solid HE under low-velocity impacts. Paper Read at the International Conference ''Shock Waves in Condensed Matter,'' Saint Petersburg, Russia, 3–8 September 2006.

[3] Nizovtsev, P. N., V. A. Rayevsky, and O. N. Ignatova. 2004. Phenomenological model of high-velocity heterogeneous straining in metals. Collective Works of RFNC-VNIIEF, Issue 7.

[4] Daridon, L., O. Oussouaddi, and S. Ahzi. 2004. Influence of the material constitutive models on the adiabatic shear band spacing: MTS, power law and Johnson-Cook models. *International Journal of Social Sciences*, 41: 3109.

[5] Bardenhagen, S. G., J. U. Brackbill, and D. L. Sulsky. 1998. Shear deformation in granular material. Paper read at the 11th International Detonation Symposium. 1998.

[6] Zerilli, F. J., R. H. Guirguis, and C. S. Coffey. 2002. A burn model based on heating due to shear flow: Proof of principle calculations. Paper Read at the 12th International Detonation Symposium, 2002.

[7] Bennett, J. G., K. S. Haberman, J. N. Johnson, B. W. Asay, and B. F. Henson. 1998. A constitutive model for the non-shock ignition and mechanical response of high explosives. *Journal of the Mechanics and Physics of Solids*, 46(12): 2303–2322.

[8] Bakhrakh, S. M., S. V. Velichko, V. F. Spiridonov et al. 2004. LEGAK-3D code for 3D time-dependant multi-material continuum flows and the ideas of its implementation on distributed-memory multiprocessors. *Voprosy Atomnoy Nauki I Tekhniki, Ser.: Math. Model. Phys. Process*, 4: 41–50.